

January 1997

NMR and Vortex Lattice Melting in $\text{YBa}_2\text{Cu}_3\text{O}_7$

Charles H. Recchia

J A. Martindale

C H. Pennington

W L. Hults

J L. Smith

Follow this and additional works at: <http://digitalcommons.wpi.edu/physics-pubs>



Part of the [Condensed Matter Physics Commons](#)

Suggested Citation

Recchia, Charles H. , Martindale, J A. , Pennington, C H. , Hults, W L. , Smith, J L. (1997). NMR and Vortex Lattice Melting in $\text{YBa}_2\text{Cu}_3\text{O}_7$. *Physical Review Letters*, 3543-.

Retrieved from: <http://digitalcommons.wpi.edu/physics-pubs/7>

NMR and Vortex Lattice Melting in $\text{YBa}_2\text{Cu}_3\text{O}_7$

C. H. Recchia,¹ J. A. Martindale,¹ C. H. Pennington,¹ W. L. Hults,² and J. L. Smith²

¹Department of Physics, The Ohio State University, 174 W. 18th Ave, Columbus, Ohio 43210

²Los Alamos National Laboratory, Los Alamos, New Mexico 87545

(Received 16 July 1996)

We report ^{89}Y and ^{17}O NMR (9 T) echo decays for $\text{YBa}_2\text{Cu}_3\text{O}_7$ and correct for contributions from dipolar coupling $^{63,65}\text{Cu}$ in order to isolate effects of vortex dynamics. We confirm vortex localization in the solid state with rms displacements consistent with Langevin dynamical theory, but with motional dynamics at time scales (10–100 μs) some $\sim 10^6$ times slower than predicted. Vortex migration over longer time scales is restricted to distances less than 1/100 of an intervortex spacing over times as long as 100 ms, in contrast with the rapid long range diffusion occurring in the liquid state. [S0031-9007(97)03068-8]

PACS numbers: 74.60.Ge, 74.25.Nf, 76.60.Lz

NMR echo decay techniques are promising tools for addressing vortex dynamics in high T_c superconductors. Such techniques have already proved valuable in problems of diffusion and flow in charge density wave conductors [1], fluids in porous media, and even in living systems [2]. In high T_c materials, however, multiple mechanisms may influence the echo decays.

In this Letter we report ^{89}Y and ^{17}O echo measurements on $\text{YBa}_2\text{Cu}_3\text{O}_7$ at 9 T. Our results are fully corrected to remove the effects of heteronuclear dipole coupling, so that effects of vortex dynamics are isolated. The correction reveals a sharp onset of echo decay effects at the melting temperature not observed in previous work [3,4], and enables direct comparison with predictions from Langevin dynamical theory. We demonstrate vortex localization for the vortex solid state with rms displacements consistent with theory, but remarkably, with motional dynamics at time scales (10–100 μs) some $\sim 10^6$ times slower than predicted in the absence of pinning. Finally, we confirm that motion persisting over yet longer time scales is severely restricted.

Aligned powder samples (~ 700 mg) of ^{17}O enriched $\text{YBa}_2\text{Cu}_3\text{O}_7$ were prepared [5] with onset T_c of 92.2 K and narrow transition (70% of maximum shielding at 87 K). The Carr-Purcell-Meiboom-Gill technique was used to enhance the ^{89}Y signal. Gyromagnetic ratios γ are $2\pi \times 577$ Hz/G (^{17}O) and $2\pi \times 209$ Hz/G (^{89}Y).

Figure 1 shows the ^{89}Y transverse relaxation rate $1/T_2$ vs T , for three orientations (0° , 45° , and 90°) of the static field (9.0 T) with respect to the sample c axis. The T_2 time characterizes the decay of the spin echo height as a function of twice the spacing τ between the applied 90° and 180° rf pulses; the decay is not exponential in all cases, but T_2 is the time at which the echo height decays to $1/e$ times its value for $2\tau = 0$. The results are in agreement with those of Suh *et al.* [3], where they report for 0° and 90° orientations; $1/T_2$ vs T exhibits a striking peak feature for $T < T_c$. A modest peak occurs for the 45° orientation. Suh *et al.* [3] attribute the peaks to vortex dynamic effects.

One must consider, however, relaxation mechanisms unrelated to vortex dynamics. Walstedt *et al.* [6] (WC) identified the dominant normal state T_2 mechanism for ^{17}O in $\text{La}_{1-x}\text{Sr}_x\text{CuO}_4$. T_2 decay requires that the nucleus experience a magnetic field contribution (parallel to the static applied field H_0) which fluctuates in time. WC

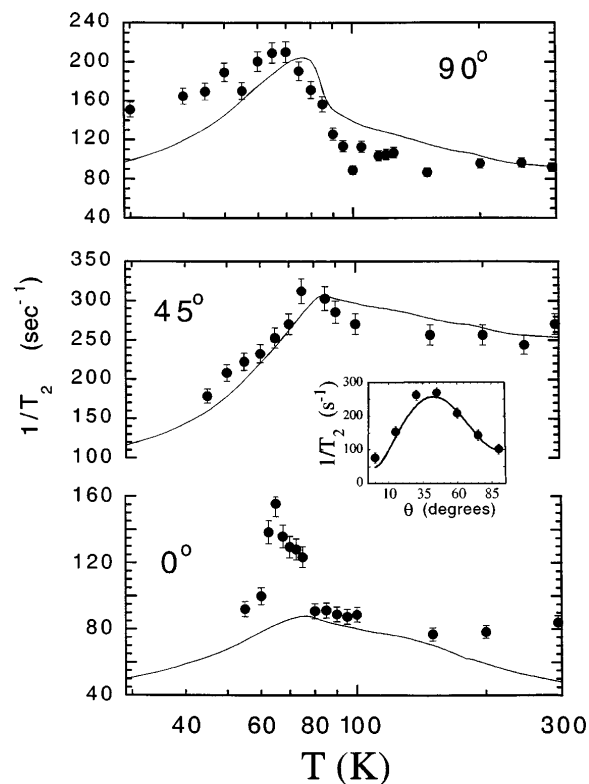


FIG. 1. ^{89}Y transverse relaxation rate $1/T_2$ vs temperature for magnetic field orientations parallel (0°), at 45° , and perpendicular (90°) to the c axis of the aligned powder $\text{YBa}_2\text{Cu}_3\text{O}_{7-\delta}$ sample ($T_c = 93$ K) at zero field, ~ 90 K in the applied field of 9 T. The theoretical curves shown are discussed in the text. Inset: room temperature (292 K) ^{89}Y $1/T_2$ vs field orientation, and curve calculated from Cu-Y dipolar interaction.

identified dipolar fields from the $^{63,65}\text{Cu}$ nuclear spins as the field source responsible for ^{17}O $1/T_2$, and the Cu T_1 transitions as the mechanism of field fluctuation. We recently [7] derived for the WC mechanism the following approximate but highly accurate analytic expression for the ^{89}Y spin echo height M as a function of pulse spacing τ :

$$M = M_0 \exp \left\{ - {}^{89}\gamma^2 \sum_{i=1}^v \left[\frac{{}^{63,65}\gamma \hbar}{r_i^3} (1 - 3 \cos^2 \theta_i) \right]^2 \right. \\ \times \frac{I(I+1)}{3(2I+1)} (T_1^{(i)})(2\tau)/T_1^{(i)} \\ \left. + 4e^{-(2\tau)/2T_1^{(i)}} - e^{-(2\tau)/T_1^{(i)}} - 3 \right\}. \quad (1)$$

The sum is taken over all Cu neighbors of Y, r_i is the Y-Cu distance, θ_i is the angle made between the applied field and the Y-Cu axis, $T_1^{(i)}$ is the T_1 of the i th Cu nucleus, and I is the Cu nuclear spin ($3/2$).

Equation (1) predicts that $^{89}(1/T_2)$ will depend on both temperature, through the measured T dependence of the ^{63}Cu T_1 [8,9], and field orientation. Figure 1 (inset) shows the measured room temperature orientational dependence of $^{89}(1/T_2)$, along with prediction of Eq. (1), with *no adjustable parameters*. The excellent agreement unambiguously specifies the WC mechanism of normal state ^{89}Y T_2 relaxation.

Figure 1 also gives the predicted temperature dependence of $^{89}(1/T_2)$ from the WC mechanism. For the 45° and 90° orientations the prediction matches the experiment remarkably well, including the peak just below T_c for the 90° orientation—Suh *et al.* [3] attributed this peak to vortex dynamic effects, but now it is clear that such effects are not necessary. Only for the $\theta = 0^\circ$ orientation is there a peak in $1/T_2$ not predicted from the WC mechanism; we present that this peak does indeed result from vortex dynamics.

Figure 2 shows measured $1/T_2$ for CuO_2 planar ^{17}O with the field parallel to c , along with several theoretical curves. The long dashed curve is calculated from the well-known “Redfield” mechanism of T_2 [10,11], using the measured ^{17}O T_1 's [8,12]. The dot-dashed curve results from the WC mechanism only, using an expression analogous to (1). The short-dashed curve combines the WC and Redfield mechanisms but still lies below experiment.

In order to match the theory with experiment in the normal state, we must invoke effects of indirect $^{63,65}\text{Cu}$ - ^{17}O nuclear coupling, mediated by the Cu electron spins [6,10,13]. We model the effect as a temperature independent enhancement of the effective Cu- ^{17}O dipolar coupling strength, with an enhancement factor of 1.58, chosen to match theory and experiment at room temperature. The resulting curve (solid) reproduces the experimental T dependence remarkably well, with the exception that it fails to predict peaks in $1/T_2$ centered at ~ 70 and ~ 30 K—note that an unpredicted peak at ~ 70 K [14] occurs for ^{89}Y as well.

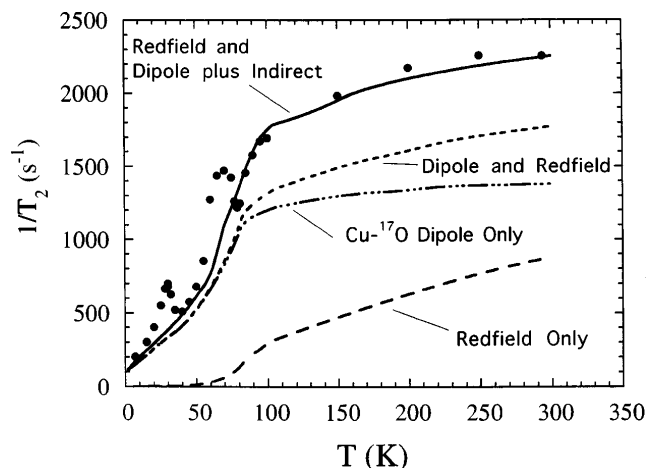


FIG. 2. Planar ^{17}O $1/T_2$ vs T for field parallel to c , with theoretical curves described in the text.

Taking the parameters of Millis-Monien-Pines (MMP) [15], one estimates [13] a nearest neighbor Cu-O indirect coupling which is $\sim 12\%$ of the near neighbor dipolar term; thus the required value of 58% is surprisingly strong. WC, in contrast, find that Cu-O indirect coupling is negligible in $\text{La}_{2-x}\text{Sr}_x\text{CuO}_4$.

Now we return to the “peaks” in the ^{17}O and ^{89}Y $1/T_2$ data (Figs. 1 and 2) which occur below T_c and which are not predicted from the WC, indirect, and Redfield mechanisms. We extract the “extra” relaxation by comparing the experimental decay curves $M(2\tau)$ at each temperature with the theoretical $M_{\text{th}}(2\tau)$ as follows:

$$M(2\tau) = M_{\text{th}}(2\tau) \exp[-2\tau(1/T_2)_{\text{extra}}], \quad (2)$$

with an adjustable $(1/T_2)_{\text{extra}}$. Experiment confirms the functional form [Eq. (2)] chosen; ^{17}O curves, which are crudely Gaussian above 76 K, are nearly exponential at 70 K, where the extra relaxation mechanism dominates. Figure 3 shows, for ^{17}O and ^{89}Y , with H_0 parallel to c , the extra relaxation $(1/T_2)_{\text{extra}}$ divided by the respective squared gyromagnetic ratio γ^2 . The ^{89}Y and ^{17}O data are in remarkable agreement. Two extra peaks are observed for ^{17}O , one at ~ 30 K and one at ~ 70 K.

The peak at 30 K is not understood; similar peaks have been observed near 35 K in $^{63}\text{Cu}(2)$ and $^{63}\text{Cu}(1)$ nuclear quadrupole resonance (NQR) T_2 experiments [16–18] at *zero applied field*; thus the peak is probably *not* related to vortices, and we make no further speculations.

Two items demonstrate that the peak at 70 K is associated with vortex dynamics. First, the peak begins its ascent from zero only below ~ 76 K, the temperature at which resistivity fully vanishes for this applied field (identified as the melting temperature T_m) [19]. It is widely believed that, above the vortex melting temperature, vortex motion is so rapid and of such large amplitude that the vortex dynamic effects on NMR are “motionally averaged” to zero; [19–23] this is also confirmed in Fig. 3 (inset), showing that the ^{89}Y inhomogeneous linewidth retains its normal state value until T is

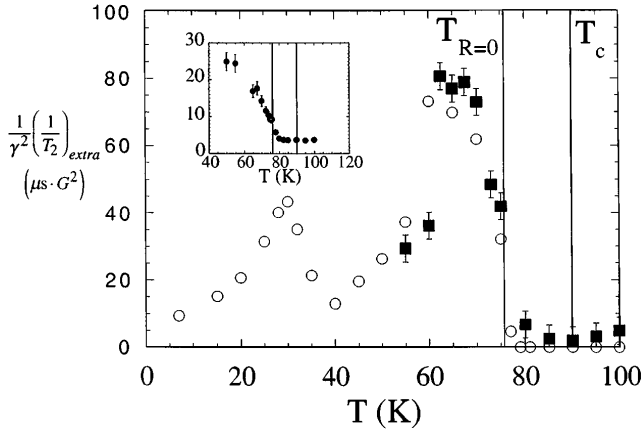


FIG. 3. Measured extra contribution to $1/T_2$, divided by the squared nuclear gyromagnetic ratios γ^2 vs T , for ^{17}O (open circles) and ^{89}Y (filled squares) with field orientation parallel to c . Vertical lines label, for the applied field of 9 T, T_c (90 K) and $T_{R=0}$ (76 K), where resistance vanishes. Inset: ^{89}Y linewidth (square root of the second moment), in Gauss, vs T with the magnetic field oriented parallel to the c axis.

below ~ 76 K. Second, ^{17}O and ^{89}Y display the same $(\gamma^2 T_2)_{\text{extra}}^{-1}$ (both magnitude and T dependence). Only a vortex dynamics mechanism can explain this, unless it is a remarkable coincidence.

What can be said quantitatively, from Fig. 3, about vortex motion? To gain insight on the spin echo we follow the “Gaussian phase approximation” [7,24,25] formalisms based on the approach of Anderson *et al.* [26]. We postulate that superposed upon the applied field H_0 is a much smaller fluctuation field $h_z(t)$ (parallel to the static field), having a time average value of zero and a mean square value $\langle h_z^2 \rangle$. $h_z(t)$ parametrizes the time variation of the local field experienced by a nucleus due to vortex motion. We further suppose that the time dependence of h_z can be described statistically according to a correlation function $\langle h_z(0)h_z(t) \rangle = \langle h_z^2 \rangle \exp(-t/\tau_c)$ with correlation time τ_c . This yields the following expression for the spin echo height as a function of pulse spacing τ [7,24,25]:

$$M_{\text{spin-echo}} = M_0 \exp[-\gamma^2 \langle h_z^2 \rangle \tau_c^2 \{2\tau/\tau_c + 4e^{-2\tau/2\tau_c} - e^{-2\tau/\tau_c} - 3\}]. \quad (3)$$

Two limits are considered, the short (4a) and long (4b) correlation time limits,

$$M_{\text{spin-echo}} \approx M_0 \exp[-(\gamma^2 \langle h_z^2 \rangle \tau_c) 2\tau] \quad \text{for } \gamma^2 \langle h_z^2 \rangle \tau_c^2 \ll 1, \quad \tau_c \ll T_2, \quad (4a)$$

$$M_{\text{spin-echo}} \approx M_0 \exp\left[-\frac{1}{12} \gamma^2 \langle h_z^2 \rangle \tau_c^{-1} (2\tau)^3\right] \quad \text{for } \gamma^2 \langle h_z^2 \rangle \tau_c^2 \gg 1, \quad \tau_c \gg T_2. \quad (4b)$$

(In defining the limits we use the fact that the values of τ chosen are typically of the order of the measured T_2 , the $1/e$ decay time.) The long correlation time limit

(4b) predicts that $1/T_2$ should scale for different nuclei as $\gamma^{2/3}$. This limit is assumed by Suh *et al.* [3], who model the system in terms of unrestricted vortex diffusion [27]. Figure 3, though, demonstrates that $1/T_2$ scales with γ^2 , not $\gamma^{2/3}$, thus specifying the short correlation time limit [Eq. (4a)]. Additionally, the functional form of the measured extra decay is in much better agreement with the exponential form of (4a). Thus, the short correlation time limit applied, specifying that $\tau_c \ll {}^{17}\text{T}_2 \approx 10^{-3}$ s, and that one may calculate $1/T_2$ from (4a):

$$1/T_2 \approx \gamma^2 \langle h_z^2 \rangle \tau_c. \quad (5)$$

The absence of motional narrowing at 70 K further specifies that $\langle h_z^2 \rangle^{1/2}$ must be much less than the measured rms linewidth of 10 G (taken from Fig. 3, inset)— $\langle h_z^2 \rangle^{1/2} \ll 10$ G—so from Eq. (5), and from the experimental $1/T_2$, we have $\tau_c \gg 10^{-6}$ s. Combining the two limits on τ_c gives $10^{-6} \ll \tau_c \ll 10^{-3}$ s. Corresponding limits on $\langle h_z^2 \rangle^{1/2}$ are $0.3 \ll \langle h_z^2 \rangle^{1/2} \ll 10$ G, and corresponding vortex displacement distances (in units of intervortex spacing) are estimated as $\langle x^2 \rangle^{1/2} \approx \langle h_z^2 \rangle^{1/2} / [2(10 \text{ G})]$, giving $0.02 \ll \langle x^2 \rangle^{1/2} \ll 0.5$. This range is of the order of typical Lindemann parameters, quite appropriate for this temperature, $T \approx T_m$, and confirms the *restriction* of vortex motion.

T_2 relevant parameters may be estimated from Monte Carlo simulations using Langevin dynamics, reported by Ryu and Stroud [22]. They simulate vortex motion in $\text{YBa}_2\text{Cu}_3\text{O}_7$ just below melting ($T \sim 0.9T_m$) and in a strong field parallel to c . Their results indicate a confinement of vortices over very long time scales within effective restriction radii of approximately 0.1 intervortex spacings, consistent with our findings. The dynamics of the motion are parametrized by a Langevin time scale τ_0 , estimated using the normal state resistivity and $B_{c2}(T)$. We used their calculations and estimated τ_0 to estimate our τ_c , but find that the resulting value is some 10^6 times shorter than required by the experiment. The very slow time scale apparent in the NMR experiment may reflect pinning effects. It is also possible that the slow motion observed is superposed upon the more rapid motion predicted, which would be transparent in the NMR experiment.

Stimulated echo experiments are effective tools for measuring diffusion, as in, for example, the diffusion of water molecules confined within biological cells [2]. We apply the three pulse stimulated echo sequence as follows: 90- τ -90- T -90- τ -echo, using fixed values of τ , 120 μs (^{17}O) and 2 ms (^{89}Y), and T values ranging from 10^{-5} to 1 s. (In fact, we use a variant of the stimulated echo, the “OE-CTPG” sequence of Ref. [28], to control for the effects of ^{17}O T_1 decay during the time T .)

Figure 4 shows the stimulated echo height vs the time T for ^{17}O and ^{89}Y at 100 and 70 K and a fixed value of τ , 2 ms for ^{89}Y and 120 μs for ^{17}O , for H_0 parallel to c . Also shown are theoretical calculations of the decay, derived analogously to Eq. (1) [7] using the WC

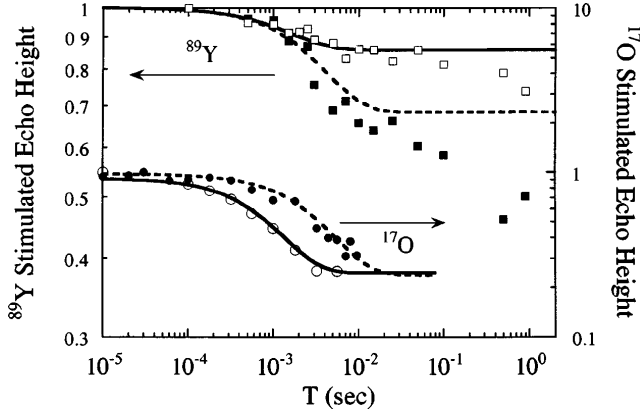


FIG. 4. Decay of the stimulated echo height vs the spacing T between the second and third pulses in the stimulated echo sequence, for ^{89}Y (squares) and ^{17}O (circles) at temperatures 100 K (open symbols) and 70 K (filled symbols). Theoretical curves, discussed in the text, are calculated for 100 K (solid curve) and 70 K (dashed curve).

mechanism *only*, with no adjustable parameters. The $\text{Cu-}^{17}\text{O}$ indirect coupling strength used is the same as that used in Fig. 2. The WC mechanism fully predicts the data, out to times of order 0.1 s, for both ^{17}O and ^{89}Y , and for both normal and superconducting states, including the temperature 70 K, where $(1/T_2)_{\text{extra}}$ reached a maximum (Fig. 3). Thus, *the stimulated echo shows no effects of vortex dynamics*.

To understand the data we return to the Gaussian phase approximation [7,24], which yields the following expression for the stimulated echo height, valid for *fixed* τ values and variable time T , and after correcting for the WC mechanism:

$$M_{\text{spin-echo}}(T) \propto \exp \left[-\gamma^2 \langle h_z^2 \rangle \tau_c^2 (2e^{-\tau/\tau_c} - e^{-\tau/\tau_c} - 1)e^{-T/\tau_c} \right] \times \exp \left[-\gamma^2 \langle h_z'^2 \rangle \tau_c'^2 (2e^{-\tau/\tau_c'} - e^{-\tau/\tau_c'} - 1)e^{-T/\tau_c'} \right]. \quad (6)$$

$\langle h_z^2 \rangle$ and τ_c are the strength and correlation time for the field fluctuation identified in the spin echo experiment. Since we have shown that $\gamma^2 \langle h_z^2 \rangle \tau_c^2 \ll 1$, Eq. (6) shows that this mechanism should not impact our stimulated echo measurements. $\langle h_z'^2 \rangle$ and τ_c' are analogous quantities for a hypothesized *additional* field fluctuation occurring over longer time scales, with $\gamma^2 \langle h_z'^2 \rangle \tau_c'^2 \gg 1$. The absence of decay beyond the WC prediction thus demonstrates that these hypothesized fluctuations are not present.

Specifically, from (6) and from the experimental data, one can show that vortex displacements occurring and persisting, in a time averaged sense, over time scales

$\tau_c' \approx 100$ ms must have $\gamma^2 \langle h_z'^2 \rangle \tau_c'^2 \ll 1$, implying displacement magnitudes much smaller than 1/100 of an intervortex spacing. Further, any displacements of amplitude of 0.1 intervortex spacings or more must persist only for time scales much less than 1 ms; such rapid, small amplitude motions are precisely what is observed as “ $1/T_2\text{-extra}$ ” in the spin echo experiment.

Results presented for $T \sim 0.9T_m$ confirm a restricted range of vortex motion with restriction radius $10^{-1 \pm 0.7}$ intervortex spacings, and τ_c , the time required to sample such a distance of $10^{-4.5 \pm 1.5}$ s, some 6 orders of magnitude slower than predicted theoretically in the absence of pinning. Vortex motion persisting over still longer time scales is *severely* restricted. Motional narrowing effects observed above T_m imply rapid vortex motion over lengths much greater than the intervortex spacing—the behaviors above and below T_m contrast starkly.

We acknowledge helpful discussions with S. Ryu, D.G. Stroud, and T.R. Lemberger. This work was supported by the U.S. Department of Energy, Midwest Superconductivity Consortium, under Contract No. DE-FG02-90ER45427.

- [1] J.H. Ross *et al.*, Phys. Rev. Lett. **56**, 663 (1986).
- [2] P.T. Callaghan, *Principles of Nuclear Magnetic Resonance Microscopy* (Clarendon Press, Oxford, 1991).
- [3] B.J. Suh *et al.*, Phys. Rev. Lett. **71**, 3011 (1993).
- [4] Y.-Q. Song, Phys. Rev. Lett. **75**, 2008 (1995).
- [5] J.A. Martindale *et al.*, Phys. Rev. B **50**, 13 645 (1994).
- [6] R.E. Walstedt *et al.*, Phys. Rev. B **51**, 3163 (1995).
- [7] C.H. Recchia *et al.*, Phys. Rev. B **54**, 4207 (1996).
- [8] P.C. Hammel *et al.*, Phys. Rev. Lett. **63**, 1992 (1989).
- [9] S.E. Barrett *et al.*, Phys. Rev. Lett. **66**, 108 (1991).
- [10] C.H. Pennington *et al.*, Phys. Rev. B **39**, 274 (1989).
- [11] C.P. Slichter, *Principles of Magnetic Resonance* (Springer, New York, 1989), 3rd ed.
- [12] J.A. Martindale *et al.*, (to be published).
- [13] C.H. Pennington *et al.*, Phys. Rev. Lett. **66**, 381 (1991).
- [14] The 70 K peak in $^{17}(1/T_2)$ has been reported by H.N. Bachman *et al.*, [Bull. Am. Phys. Soc. **41**, 467 (1996)].
- [15] A.J. Millis *et al.*, Phys. Rev. B **42**, 167 (1990).
- [16] A.V. Bondar *et al.*, JETP Lett. **50**, 146 (1989).
- [17] K. Kumagai *et al.*, J. Phys. Soc. Jpn. **59**, 2336 (1990).
- [18] Y. Itoh *et al.*, J. Phys. Soc. Jpn. **59**, 3463 (1990).
- [19] C.H. Recchia *et al.*, Phys. Rev. B **52**, 9746 (1995).
- [20] H.B. Brom and H. Alloul, Physica (Amsterdam) **177C**, 297 (1991).
- [21] S.L. Lee *et al.*, Phys. Rev. Lett. **71**, 3862 (1993).
- [22] S. Ryu and D.G. Stroud, Phys. Rev. B **54**, 1320 (1996).
- [23] P. Carretta *et al.*, Phys. Rev. Lett. **68**, 1236 (1992).
- [24] A. Abragam, *Principles of Nuclear Magnetism* (Clarendon Press, Oxford, 1961) (reprinted 1989), Chap. 10.
- [25] B. Herzog *et al.*, Phys. Rev. **103**, 148 (1956).
- [26] P.W. Anderson *et al.*, Rev. Mod. Phys. **25**, 269 (1953).
- [27] Here we adapt their analysis to the framework of Eq. (4b), identifying their DG^2 with our $\langle h_z^2 \rangle \tau_c^{-1}$.
- [28] T.J. Norwood, J. Magn. Reson. A **103**, 258 (1993).